Two-Phase Vessel Blowdown of an Initially Saturated Liquid—Part 2: Analytical

M. N. Hutcherson
Senior Mechanical Engineer.
Assoc. Mem ASME

R. E. Henry
Vice President.

Fauske and Associates, Inc.,
Burr Ridge, Ill. 60521

D. E. Wollersheim
Professor,
Mechanical Engineering Department,
University of Missouri,
Columbia, Mo.

Analytical models are presented to predict the internal vessel conditions during the decompression regimes of an initially saturated liquid. A subcooled blowdown analysis considers the elasticity of both the liquid and vessel. A bubble growth analysis for the intermediate period of blowdown is based on thermally dominated bubble growth from a solid surface into a superheated liquid. A dispersed analysis for the latter decompression period assumes the vapor bubbles have grown sufficiently so the liquid is uniformly distributed within the vapor phase. The subcooled analysis predicts the initial period of blowdown reasonably well. The bubble growth analysis predicts the rise in system pressure above that value to which it initially falls after the end of subcooled blowdown. It considers an initially "slow" depressurization rate (less than 400 MPa/s) where nucleation and bubble growth is the dominate volume producing, and thus pressure recovery, mechanism. It provides insight into why the system pressure initially drops below the saturation pressure, and it also offers an explanation for the subsequent recovery of the system pressure toward the saturation pressure. The thermodynamic equilibrium analysis provides a reasonable prediction of the latter stage of decompression. The combination of these three models predicts the overall two-phase decompression phenomenon reasonably well.

1 Introduction

This study addresses the thermodynamic and fluid dynamic aspects of two-phase blowdown of a high pressure-temperature fluid from an initial subcooled or saturated liquid state. Blowdown analysis combines a description of both the thermal-fluid behavior inside the blowdown vessel in addition to the escape flow limiting mechanism from the system. The behavior inside the blowdown vessel controls the fluid compressibility at the entrance to the exhause duct $P_{T,e}$, x_e). Hence, it controls the critical flow condition from the system and thus the depressurization rate. The two-phase blowdown phenomenon has applicability to boilers, refrigeration and cryogenic systems, chemical systems, railroad tank car transportation [1], and boiling and pressurized water nuclear reactors. It is the later, nuclear reactor safety, which has provided the primary impetus to more fully understand the two-phase decompression phenomenon. The analyses presented herein are a summary of a larger study [2]. It addressed among other questions the existence, magnitude, and effect of metastable thermodynamic states on two phase blowdown.

Metastable thermodynamic states, namely superheated liquid, exist in the early stage of decompression from an initially subcooled or saturated liquid condition [2–8]. Recent emphasis [9–10] has been to more fully understand the vapor generation (nucleation) mechanism as a result of boiling and/or flashing. Recent studies have also indicated that the nucleation mechanism at the start of subcooled and saturated liquid blowdown depends on the initial rate of pressure decay [11]. It is suggested that such blowdowns can be classified as either "fast" or "slow," depending on this criteria (normally taken to be about 400 MPa/s). Following this type classification, the decompressions reported in this study fall into the "slow" category in which nucleation from solid surfaces which contain imperfections (nucleation sites) is dominate. The effect of the magnitude of the nucleation process in the early stage of a "slow" blowdown is largely dependent on the internal vessel geometry. It is primarily related to the (*i*) internal interfacial surface area between liquid and solid surface, (*ii*) initial internal volume of liquid, (*iii*) break flow area from the system, (*iv*) internal flow area within the system, and (*v*) the location of the break in the system. A complete thermodynamic equilibrium analysis of the phenomenon [12] does not account for the superheated liquid condition at the start of blowdown. Consequently, it does not adequately describe the overall phenomenon. Even though this approach does not completely describe the phenomenon in the general case, it does become more representative of slower decompressions. Many blowdown analyses to date [13–18] has been performed in a thermodynamic equilibrium manner for the entire decompression. However, this is not a completely valid assumption [7]. Nucleation at the start of blowdown is initiated primarily from the activated surface cavities at the internal solid-liquid interfaces. It does not predominantly occur in the bulk liquid [19]. There is a fraction of the spectrum of internal surface cavities which are not flooded during heat-up and which are larger than minimum embryo size. These can subsequently function as nucleation sites upon decompression. Most initially two-phase critical flow models to date have also assumed that the expanding two-phase mixture behaves in an ideal, thermodynamic equilibrium manner. However, recently the merits of nonequilibrium critical flow analysis [20] have been recognized and implemented. There has been considerable experimental effort directed toward understanding the overall two-phase decompression phenomenon in a reactor system. This work includes that of Semiscale and LOFT, [21–24], Battelle [25, 26] (U.S. and Germany), Japan [27], and Marviken [28].

The objectives of the analytical portion of this study were primarily to understand (*i*) the transition from subcooled blowdown to the initiation of nucleation, (*ii*) the influence of the nucleation process on the early stage of decompression, and (*iii*) the transition from the bubble growth to dispersed stage of blowdown.

Contributed by the Heat Transfer Division for publication in the JOURNAL OF HEAT TRANSFER. Manuscript received by the Heat Transfer Division January 12, 1982.

2 Analysis

The two-phase decompression scenario should be divided into at least two different major classes of related phenomena [6]. The first is the fluid behavior inside the blowdown vessel upstream of the entrance to the exhaust duct, and the second is the fluid behavior inside the exhaust duct itself. The fluid behavior inside the vessel establishes the flow pattern and local fluid quality at the entrance to the exhaust duct. The presence of structure within the vessel can also significantly effect the internal flow regime. Internal structure also markedly impacts the very early stage of decompressoin by supplying additional potentially active surface cavities. These can serve as nucleation sites for the inception of vaporization. The history of previous fluid and wall pressure-temperature conditions within the vessel also effects the inception of vaporization upon depressurization. Analytical models are described herein for each of the three major decompression regimes: subcooled, bubble growth, and dispersed.

2.1 Subcooled Model. The initial period of blowdown when the fluid in the system is subcooled liquid is analyzed in this section. The assumptions employed in this model are as follows:

(*a*) The system is instantaneously opened to the ambient.

(*b*) There is frictionless, one-dimensional flow in a smooth entrance exhaust duct.

(*c*) The exhaust duct has a constant cross sectional area and internal volume.

(*d*) The flow is initially unchoked and subsequently becomes choked.

(*e*) The vessel material is elastic.

The accelerating (inertial) flow period at the start of blowdown when the flow is subcritical is small compared to the overall subcooled decompression period. It only lasts for a few milliseconds. Hence, the exhaust flow is choked during virtually all of subcooled blowdown.

The transient, subcritical flow rate in the early stage of subcooled blowdown can be described as

$$G(t) = \frac{C_d}{L}\left[P_{T,e}(t) - P_a\right]t \tag{1}$$

When the transient flow rate in (1) increases to the critical flow rate, the flow is assumed to become choked at the exit of the exhaust duct. The critical flow rate and critical exit pressure can then be determined from an initially subcooled and saturated liquid critical flow model. Such a model [29] must be evaluated at the instantaneous total thermodynamic conditions at the entrance to the exhaust duct ($P_{T,e}$, $T_{T,e}$). During this period, the thermodynamic state of the remaining fluid within the vessel is subcooled liquid. However, the state of the fluid in the exhaust duct is a compressible, two-phase, liquid-vapor mixture. It is the behavior of this compressible, two-phase, liquid-vapor mixture in the exhaust duct which limits the escape flow rate from the system.

The system response during the subcooled period of decompression is analyzed as follows. A conservation of mass in the vessel during the blowdown is

$$\frac{dm_l}{dt} = -GA_x \tag{2}$$

Equation (2) can be integrated initially with the subcritical flow rate, (1), and subsequently with the critical flow rate. The specific volume of the remaining liquid within the system is then

$$v_l = \frac{V_T}{m_l} \tag{3}$$

the influence of the elasticity of the vessel material on the subcooled blowdown is accounted for by considering the hoop stress in a thin walled vessel. This is given by

$$\sigma = \frac{1}{2\delta}\left[P_{T,e}d - P_a(d+2\delta)\right] \tag{4}$$

The vessel material is assumed to be described by Hookes Law in the elastic range. Differentiating the relation for the internal volume of a cylindrical vessel produces

$$dV_T = 2V_T\frac{dr}{r} \tag{5}$$

Equations (4) and (5) may be combined to determine the change in the original, unstressed vessel volume.

Equation (3) can be differentiated to produce

$$\frac{dv_l}{dt} = \frac{1}{m_l}\frac{dV_T}{dt} - \frac{V_T}{m_l^2}\frac{dm_l}{dt} \tag{6}$$

Nomenclature

A = cross-sectional flow area
α = void fraction, thermal diffusivity
C = coefficient, degrees Centigrade
c = specific heat capacity
d = inside diameter of vessel
Δ = finite difference
δ = vessel wall thickness
E = elasticity
F = degrees Fahrenheit
G = mass flux, $\dot{m}/A$
g = acceleration of gravity at sea level
h = specific enthalpy
η = critical exit or throat pressure ratio
J = Joule, (N − m)
Ja = Jakob number, $c_L\rho_L\ (T - T_{sat})/\rho_V h_{VL}$
K = degrees Kelvin
L = exhaust duct length
m = mass, meter
N = number of bubbles or nucleation sites in a given generation, Newtons
P = static pressure
Pa = Pascal (N/m^2)
r = radius
ρ = density
S = surface area
s = specific entropy
σ = surface tension, normal stress
T = temperature
t = time
u = flow speed
V = volume
v = specific volume
x = fluid quality

Subscripts

a = ambient
c = choked or critical flow, thermodynamic critical state or property
d = discharge, bubble departure
e = entrance
i = initial, given sector of system
L = saturated liquid
l = subcooled liquid
max = maximum
o = stagnation
p = produced
sat = saturation
Sup = superheat
T = total, total thermodynamic property
τ = arbitrary time step from start of blowdown
τ' = time step from start of growth of current bubble generation from surface
VL = saturated vapor minus liquid thermodynamic property
V = saturated vapor
x = exit
∞ = free stream

The dm_l/dt is evaluated from (2), and the dV_T/dt is determined from the change in the volume of the vessel, (5).

The depressurization rate of the liquid remaining within the system is dependent upon its elasticity according to

$$\frac{dP}{dt} = \frac{-E_l}{v_l}\frac{dv_l}{dt} \tag{7}$$

where the dv_l/dt is determined from (6). Equations (4), (5), (6), and (7) can then be combined to determine the instantaneous internal vessel stagnation pressure during the subcooled regime of decompression.

2.2 Bubble Growth Model. The system pressure recovery phenomenon during the early stage of blowdown after the pressure has dropped below the local saturation pressure is analyzed in this section. It is postulated that the volume producing mechanism within the system is initially inertially controlled and then thermally dominated vapor bubble growth.

The internal volume of the system is considered constant so that

$$V_T = V_V + V_L = m_V v_V + m_L v_L \tag{8}$$

Equation (8) is differentiated to produce

$$\frac{dv_V}{dt} = \frac{-1}{m_V}\left[v_L\frac{dm_L}{dt} + v_V\frac{dm_V}{dt} + m_L\frac{dv_L}{dt}\right] \tag{9}$$

The factor dv_L/dt is determined from the elasticity of the liquid phase as

$$\frac{dv_L}{dt} = \frac{-1}{E_L v_L}\frac{dP}{dt} \tag{10}$$

The behavior of the saturated vapor phase is approximated as Pv_V = constant, so the left side of (9) becomes

$$\frac{dv_V}{dt} = \frac{-v_V}{P}\frac{dP}{dt} \tag{11}$$

Substituting (10) and (11) into (9) gives the following relation for the time rate of change of the internal vessel pressure

$$\frac{dP}{dt} = \frac{PE_L}{m_V v_V E_L + v_L P}\left[v_L\frac{dm_L}{dt} + v_V\left(\frac{dm_V}{dt}\right)_{\text{net}}\right] \tag{12}$$

The total mass flow rate from the system is

$$\frac{dm}{dt} = -GA_x \tag{13}$$

For homogeneous, incompressible flow, which is a good approximation during the early, low void fraction period of the blowdown, the flow rate is

$$G = \rho u = [2\rho(1-\eta_c)P_{T,e}]^{1/2} \tag{14}$$

The η_c is the saturated liquid critical exit pressure ratio, and the fluid density is

$$\rho = \rho_V\alpha + \rho_L(1-\alpha) \tag{15}$$

The mass flow rate of the liquid phase from the system is then

$$\frac{dm_L}{dt} = -\rho_L A_x(1-\alpha)\left[\frac{2(1-\eta_c)P_{T,e}}{\rho_V\alpha + \rho_L(1-\alpha)}\right]^{1/2} \tag{16}$$

and that of the vapor phase from the system is

$$\frac{dm_{V,x}}{dt} = -\rho_V A_x\alpha\left[\frac{2(1-\eta_c)P_{T,e}}{\rho_V\alpha + \rho_L(1-\alpha)}\right]^{1/2} \tag{17}$$

Equation (16) can be substituted directly into (12). However, the change in the mass of the vapor phase within the system in (12) is a net difference. It is the result of the production of vapor mass by bubble nucleation minus the rate of vapor mass exhausted from the system (17).

The inertially dominated bubble growth period given by

$$r = \left\{\frac{2}{3}v_l[P_{\text{sat}}(T) - P_l]\right\}^{1/2} t \tag{18}$$

is very short for most fluids. It was approximately 10^{-8} s in the tests reported in this study. Thus, the bubble growth is assumed to be primarily thermally controlled as given by

$$r = \left[\frac{12}{\pi}\alpha_l \text{Ja}\right]^{1/2} t^{1/2} \tag{19}$$

where the Jakob number, Ja, is

$$\text{Ja} = \frac{c_L\rho_L(T - T_{\text{sat}})}{\rho_V h_{VL}} \tag{20}$$

The volume of an individual spherical bubble growing in a thermally dominated manner (19) is

$$V_b = \frac{4}{3}\pi\left[\frac{12}{\pi}\alpha_l \text{Ja}^2\right]^{3/2} t^{3/2} \tag{21}$$

where (t) is the time for inception.

The departure diameter of steam bubbles growing from a surface in pool boiling conditions has been correlated [30] as

$$D_d = 1.5\times 10^{-4}\left[\frac{\sigma}{g(\rho_L - \rho_V)}\right]^{1/2}\left[\frac{c_L\rho_L T_{\text{sat}}}{\rho_V h_{VL}}\right]^{5/4} \tag{22}$$

The surface tension (σ) of saturated water against its own vapor (steam) in (22) has been correlated by White [31] as

$$\sigma(N/m) = 0.2358\left[1 - \frac{T}{T_c}\right]^{1.256}\left[1 - 0.625\left(1 - \frac{T}{T_c}\right)\right] \tag{23}$$

A simplification of (23) which is within 1 percent of it over the range of 366–566 K (200–560°F) is

$$\sigma(N/m) = 0.14783\left[1 - \frac{T}{T_c}\right]^{1.053} \tag{24}$$

The departure diameter is then used in (19) to determine when a bubble will separate from the surface. By knowing the departure bubble diameter and the total surface area within the system, the maximum number of nucleation sites can be determined as

$$N_{\max} = \frac{2}{\sqrt{3}}\frac{S_T}{D_d{}^2} \tag{25}$$

This assumes that the bubbles on the wall at departure are just touching each other, spherical in shape, and arranged in a triangular array. The increasing diameter of a bubble on the wall can be determined from (19) for time greater than the inertially controlled period (18). When the diameter of the bubbles on the surface reach the departure diameter, that generation is assumed to leave the surface and continues to grow in the liquid.

The incremental vapor volume production is the increase in volume of the vapor bubbles in the free stream and also those growing from the solid surface. This is given by

$$\Delta V_{V,\tau} = \Delta V_{V,\infty,\tau} + \Delta V_{V,\omega,\tau'} \tag{26}$$

The incremental mass of vapor produced within the system can then be approximated as

$$\Delta m_{V,P,\tau} = \rho_{V,\tau}\Delta V_{V,\tau} \tag{27}$$

The net change in the mass of the vapor phase within the system is then

$$\Delta m_{V,\tau} = \Delta m_{V,P,\tau} + \Delta m_{V,x,\tau} \tag{28}$$

This net change in the mass of the vapor within the system (28), where the second term is negative, is then used in (12).

If the bubbles growing from the surface have not yet reached departure size, their growth is determined by the instantaneous Jakob number (19, 20). However, if the growing bubbles have reached departure size, they separate from the surface. The current internal vessel pressure then determines a new departure bubble diameter from (22). This then determines the current number of vapor bubbles growing from the surface in the next generatoin, (25). This analysis

then applies to the period of blowdown in which the fluid configuration remains to be vapor bubbles growing in a superheated liquid.

2.3 Dispersed Model. This section considers the liquid-vapor mixture when it closely approaches thermodynamic equilibrium conditions. This occurs when the fluid configuration in the system changes from vapor bubbles growing in a superheated liquid toward a dispersed, two-phase mixture. It is assumed that the bubbly to dispersed fluid configuration transitition occurs at a void fraction of approximately 0.3 [32]. The remaining fluid is then assumed to expand isentropically. The pressure and quality at this condition then determines the initial entropy from which the fluid expands in the dispersed regime as given by

$$s_i = s_V(P_i)x_i + s_L(P_i)(1-x_i) \tag{29}$$

For a homogeneous fluid, the quality in (29) when the fluid configuration transition occurs can be determined from

$$x_i = \frac{v_L(P_i)\alpha_i}{v_L(P_i)\alpha_i + v_V(P_i)(1-\alpha_i)} \tag{30}$$

The continuity equation for flow from the system is given in (13) when employing the critical flow rate, G_c. It can then be integrated to determine the instantaneous fluid mass remaining with the system. The two-phase critical flow rate in (13) is determined from the Henry-Fauske critical flow model [33] in this analysis. The instantaneous specific volume of the remaining mixture is determined from $v = V/m$. This specific volume can then be used to determine the homogeneous fluid quality from

$$x = \frac{V/m - v_L(P)}{v_{VL}(P)} \tag{31}$$

The remaining homogeneous mixture is assumed to expand isentropically so

$$s_i = s[P(t)] = s_V(P)x + s_L(1-x) = \text{constant} \tag{32}$$

where the fluid quality in (32) is that from (31). Equations (29), (30), (31), and (32) are then combined to determine the internal vessel pressure history during the homogeneously dispersed regime of blowdown.

3 Discussion

The proposed subcooled blowdown model compares reasonably well with measured internal vessel pressure histories as illustrated in Fig. 1. This particular test was performed in a large-scale, reactor simulator vessel which contained internal structure in the form of a separator plate. Even with this large blowdown vessel and its internal complexities, this simple model still predicted the pressure decay during the subcooled period of this blowdown reasonably well.

In the bubble growth blowdown model, vapor nuclei are assumed to originate at the wall and continue to grow while being limited by thermal conduction to the liquid-vapor interface. The bubbles are then assumed to continue to expand and pressurize the system. *The net effect of the volume production rate within and the volume escape rate from the system is then assumed to be the controlling mechanism of the system pressure.* This only applies while the fluid configuration is vapor bubbles growing in a superheated liquid, i.e., for $\alpha \leq 30$ percent [32]. This proposed model is illustrated and validated in more detail as follows.

The predicted system pressure history in the bubble growth regime of blowdown is nearly independent of the initial liquid superheat for a given system geometry. However, the predicted system pressure is more sensitive to the number of potential nucleation sites per unit surface area (N/S) for a given initial liquid superheat. Decreasing the N/S decreases the predicted pressure history. This effect on the predicted

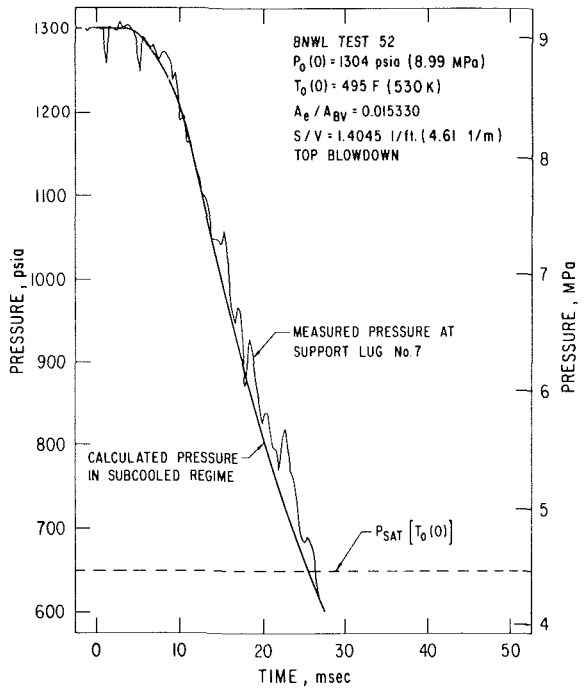

Fig. 1 Comparison of the subcooled blowdown model to the data of BNWL run 52 [25]

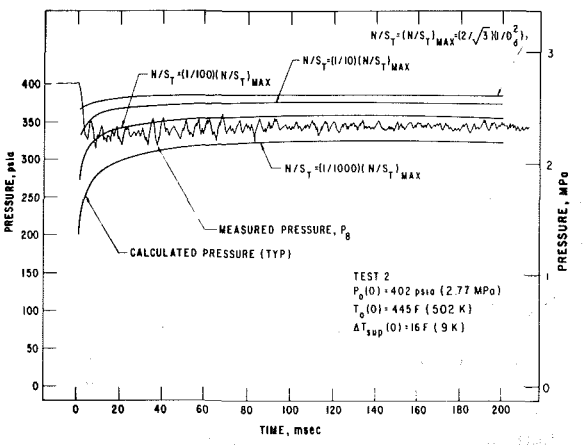

Fig. 2 Comparison of the measured and predicted internal vessel pressure by the bubble growth blowdown model for various *N/S* in test 2

pressure history for test 2 of this study is shown in Fig. 2. A range of three decades of the maximum N/S in Fig. 2 approximately brackets the measured pressure history. However, Fig. 2 illustrates that 1 percent of the maximum N/S best predicts the measured system pressure history.

The vapor volume within the system during the decompression is given by

$$V_V = V_T - mv_L \tag{33}$$

where m is the measured remaining mass inside the vessel. The predicted vapor volume within the system for 1 percent of the maximum N/S compared well with the inferred vapor volume from (33). Thus, *the vapor volume producing mechanism during the early period of the decompression appears to be thermally dominated bubble growth in a superheated liquid.*

The predicted pressure and void fraction histories in the vessel in test 2 for 1 percent of the maximum N/S are shown in Fig. 3. Since this analysis only considers bubble growth in a superheated liquid, it applies only during the period this fluid

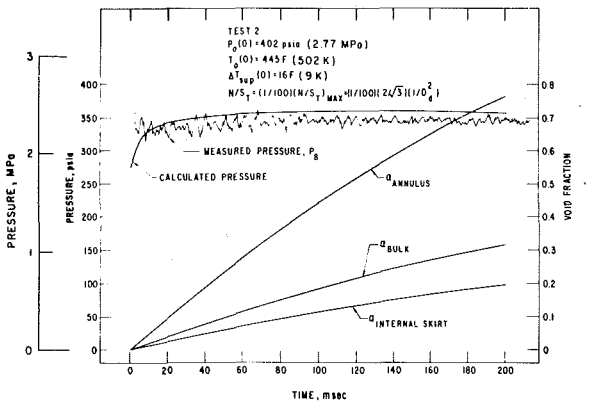

Fig. 3 Comparison of the measured and calculated internal vessel pressure by the bubble growth blowdown model in test 2

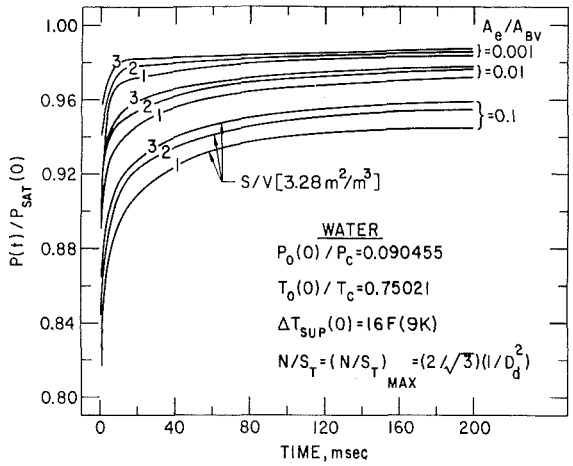

Fig. 4 Prediction of the internal vessel pressure history during the early stage of decompression by the proposed bubble growth blowdown model

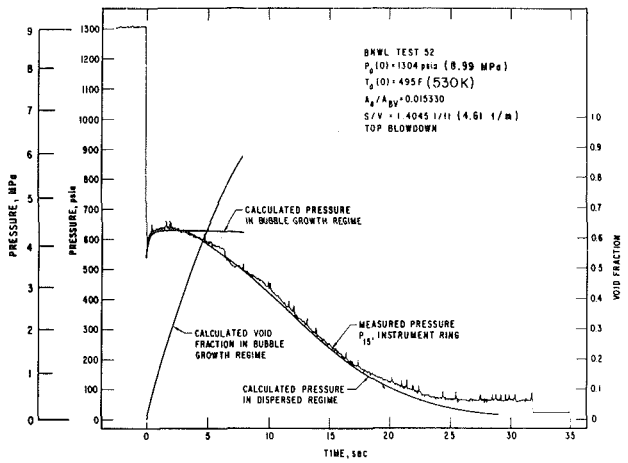

Fig. 5 Comparison of the dispersed regime blowdown model prediction to the measured pressure history of BNWL run 52 [25]

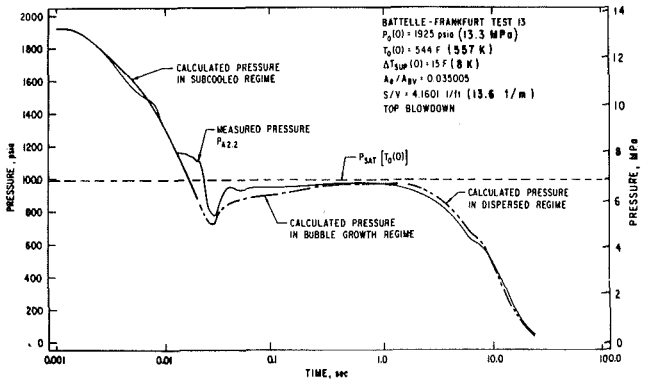

Fig. 6 Comparison of the subcooled, bubble growth, and dispersed blowdown models to the measured pressure in the Battelle-Frankfurt run 13 [26]

configuration exists during the decompression. The maximum void fraction in a bubbly fluid configuration without bubble coalescence is about 70 percent. However, in practice the bubbly fluid configuration is not sustained beyond a void fraction of approximately 30–40 percent [32]. Hence, the predictions in Fig. 3 are applicable primarily in the range of the void fraction in the downcomer annulus from zero to about 30 percent. These predictions compare well with the measured internal vessel pressure histories in this experiment. The void fraction in the downcomer annulus is used in determining the mass flow rates of the liquid and vapor phases escaping from the system. It is the best indicator of a flow regime transition in this region of the system.

The pressure during the bubble growth period of decompression is dependent upon the internal surface area and size of the exit from the system. The system pressure is greater for reduced area ratios (A_e/A_{BV}) for a given ratio of internal solid surface area per unit volume (S/V) as shown in Fig. 4. The volume of the vessel employed in this study was used for illustration. The instantaneous system pressure is also greater for increased S/V at a given area ratio. As illustrated in Fig. 4, the system pressure is more sensitive to S/V as the area ratio is increased, and the pressure also recovers slower as the area ratio is increased and S/V is decreased. The system pressure is typically more sensitive to S/V than it is to the area ratio.

This bubble growth analysis can be applied to each sector within a system during depressurization. Once the bubbly to dispersed fluid configuration transition occurs, the vaporization of superheated liquid droplets is the only remaining mechanism to sustain the pressure. This bubble growth blowdown model can also be used to predict the decompression characteristics in an initially nonisothermal system.

The proposed dispersed regime blowdown model is compared to the measured pressure history in the BNWL top blowdown run 52 [25] in Fig. 5. As illustrated, the dispersed model prediction compares well with the measured pressure history. This is particularly noteworthy considering that this model assumes a completely dispersed fluid, and this was a top blowdown which influences phase separation during blowdown [34]. Also, this dispersed regime blowdown model is based only on simple thermodynamics, and it pedicts the measurements quite well. This good agreement of model and experiment is also demonstrated in additional comparisons in this study.

The combined pressure history predictions of the three foregoing models are compared to the measured pressure history of Battelle-Frankfurt [26] run 13 in Fig. 6. The comparison is reasonably good even though the predictions deviate somewhat from the measurements at about 25 ms. This is attributed to dissolved gas coming out of solution.

4 Conclusions

The most significant conclusions drawn from the analytical portion of this study are as follows:

1 The subcooled blowdown model reasonably well predicts the early period of decompression when significant amounts

of dissolved, noncondensable gases do not come out of solution.

2 The bubble growth blowdown model predicts the recovering internal vessel pressure history after surface cavity activation when most of the remaining fluid is superheated liquid. This model indicates proper trends, and it also compares well with available data.

3 The recovering internal vessel pressure at the start of blowdown is dependent upon (*a*) the internal vessel surface area, (*b*) the internal vessel volume, (*c*) the exit or break flow area, and (*d*) the flow area within the vessel. Phase separation increases as the exit flow area decreases relative to the internal vessel flow area.

4 The recovering internal vessel pressure history at the start of decompression is more sensitive to S/V than it is to A_x/A_{BV}.

5 As the S/V decreases, the liquid in the vessel remains superheated longer, which promotes the internal vessel pressure to remain nearly constant for a longer period particularly for small A_x/A_{BV}.

6 The proposed dispersed regime blowdown model compares well with available data.

Acknowledgment

The authors acknowledge the financial support for this study from the U.S. Energy Research & Development Administration. This work was performed in the Experimental Modeling Section of the Reactor Analysis & Safety Division of Argonne National Laboratory.

References

1 Sallet, D. W., Hannemann, R. J., and Guhler, M., "An Investigation Into Unsteady Two Phase Depressurization of Vessels Through Orifices and Short Pipes," ASME 78-WA/HT-35, 1978.

2 Hutcherson, M. N., "Contribution to the Theory of the Two Phase Blowdown Phenomenon," ANL-75-82, Argonne National Laboratory, 1975; also, University Microfilms, 76-21951, 1976; and University of Missouri, Mechanical Engineering Department (Ph.D. dissertation) Columbia, Mo. 1975.

3 Edwards, A. R., and O'Brien, T. P., "Studies of Phenomena Connected With the Depressurization of Water Reactors," *Journal of Brit. Nucl. Energy Soc.*, Vol. 9, No. 2, April 1970, pp. 125-135.

4 Tanger, G. E., Vachon, R. I., and Pollard, R. B., "Pool Boiling Response to Pressure Decay," *Proc. Third Intl. Heat Transfer Conf.*, Vol. 4, 1966, pp. 38-43.

5 Brown, E. A., "Explosive Decompression of Water," *Proceedings Heat Transfer and Fluid Mechanics Inst.*, Stanford, Calif., June 15-17, 1960, pp. 135-146.

6 Hutcherson, M. N., Henry, R. E., and Wollersheim, D. E., "Two-Phase Vessel Blowdown of an Initially Saturated Liquid—Part 1: Experimental," ASME JOURNAL OF HEAT TRANSFER, Vol. 105, No. 4, pp. 687-693.

7 Winters, W. S., and Merte, H., "Experiment and Nonequilibrium Analysis of Pipe Blowdown," *Nucl. Sci. and Eng.*, Vol. 69, 1979, pp. 411-429.

8 Edwards, A. R., and Jones, C., "An Analysis of Phase IIA Blowdown Tests—the Discharge of High Enthalpy Water from a Simple Vessel into a Containment Volume," SRD-R-27, Safety and Reliability Directorate, United Kingdom Atomic Energy Authority, Warrington, Lancashire, England, 1974.

9 Leslie, D. C., "The Development of Flashing Flow from Existing Nucleation Sites," AEEW-R505, United Kingdom Atomic Energy Authority, Reactor Group, Winfrith, Dorchester, Dorset, England, 1966.

10 Hunt, D. L., "The Effect of Delayed Bubble Growth on the Depressurization of Vessels Containing High Temperature Water," Report AHSB(S)R189, United Kingdom Atomic Energy Authority, Nov. 1970.

11 Alamgir, M. D., Kan, C. Y., and Lienhard, J. H., "An Experimental Study of the Rapid Depressurization of Hot-Water," ASME JOURNAL OF HEAT TRANSFER, Vol. 102, No. 5, 1981.

12 Rasmussen, J., Rasmussen, L., Malnes, D., Imset, O., "Simulation of Blowdown from Pressure Vessels Based on Nonisothermal Equilibrium Effects. Comparison with Experimental Data," European Two Phase Flow Group Mtg., Harwell, England, June 1974.

13 Moore, K. V., and Rettig, W. H., "RELAP4-A Computer Program for Transient Thermal Hydraulic Analysis," ANCR-1137 Rev. 1, Aerojet Nucl. Co., Mar. 1975.

14 Katsma, K. R., *et al.*, "RELAP4/Mod5, A Computer Program for Transient Thermal Hydraulic Analysis of Nuclear Reactor and Related Systems," ANCR-NUREG 1335, Aerojet Nucl. Co., Sept. 1976.

15 Moore, K. V., et al., "RETRAN—A Program for One-Dimensional Transient Thermal Hydraulic Analysis of Complex Fluid Flow Systems," EPRI-NP-408, Electric Power Research Institute, Jan. 1977.

16 Gido, R. G., Grimes, C. I., Lawton, R. G., and Kudrick, J. A., "COMPARE—A Computer Program for the Transient Calculation of a System of Volumes Connected by Flowing Vents," LA-NUREG-6488-MS, also NRC-4, Los Alamos Laboratory, Sept. 1976.

17 Wheat, L. L., Wagner, R. J., Neiderauer, G. F., and Obernchain, C. G., "CONTEMPT-LT, A Computer Program for Predicting Containment Pressure-Temperature Response to a Loss of Coolant Accident," ANCR-1219, Aerojet Nucl. Co., June 1975.

18 Broadus, C. R., James, S. W., Lee, W. H., Lime, J. F., and Pate, R. A., "BEACON/Mod 2—A Program for Analyzing the Flow of Mixed Air, Steam, and Water in a Containment System," CDAP-TR-002, EGG, Dec. 1977.

19 Hoppner, G., "Experimental Study of Phenomena Affecting the Loss of Coolant Accident," Ph.D. thesis, University of California at Berkeley 1971.

20 Vigil, J. C., and Pryor, R. J., "Transient Reactor Analysis Code (TRAC) Development and Assessment," *Journal of Nucl. Safety*, Vol. 21, No. 2, Mar.-Apr. 1980.

21 Alder, R. S., Feldman, E. M., and Pinson, P. A., "Experimental Data Report for 1-1/2 Loop Semiscale System Isothermal Test 1011," ANCR-1146, Aerojet Nucl. Co., Mar. 1974.

22 Zender, S. N., Crapo, H. S., Jensen, M. F., Sackett, K. R., "Experimental Data Report for Semiscale Mod-1, Test S-01-1," ANCR-1198, Aerojet Nucl. Co., Apr. 1975.

23 Hall, D. G., "A Study of Critical Flow Prediction for Semiscale Mod-1 Loss of Coolant Accident Experiments," TREE-NUREG-1006, USNRC, Dec. 1976.

24 Prassinas, P. G., Galvsha, B. M., Jarrell, D. B., "Experimental Data Report for LOFT Nonnuclear Small Break Experiment L3-0," NUREG/CR-0959, TREE-1390, EGG Idaho, Aug. 1979.

25 Allemann, R. T., McElfresh, A. J., Neuls, A. S., Townsend, W. C., Wilburn, N. P., and Witherspoon, M. E., "Coolant Blowdown Studies of a Reactor Simulator Vessel Containing a Perforated Sieve Plate Separator," BNWL-1463, Battelle Northwest Lab., Richland, Wash., Feb. 1971.

26 Kanzleiter, T., Koehn, J., Sauberlich, C., Stein, K., and Zimmermann, M., "Untersuchung der Vorgange bei der Druckentlastung Wassergekuhlter Reaktoren," 8. Bericht, Band I, Battelle Institut, Germany, July 1971.

27 Hugie, H., Yamanauchi, A., Sagawa, N., Ogasawara, H., and Tagami, T., "Studies for Safety Analyses of Loss of Coolant Accidents in Light Water Reactors," *J. Japan Soc. Mech. Eng.*, Vol. 69, (571), Aug. 1966, p. 1068.

28 Ericsen, L., Gros Daillon, L., Hall, D., Kilpi, K., Ravnsbova, J., Sandervag, O., and Vidarsson, J., "The Marviken Full Scale Critical Flow Tests: Interim Report; Results from Tests 1-7," Marviken Power Station, Sweden.

29 Henry, R. E., "Two-Phase Critical Discharge of Initially Saturated and Subcooled Liquid," *Nucl. Sci. Eng.*, Vol. 41, 1970, p. 336.

30 Cole, R., and Rohsenow, W. M., "Correlation of Bubble Departure Diameters for Boiling of Saturated Liquids," *Chem. Eng. Prog. Sym. Series*, AIChE, Vol. 65, 1969, p. 92.

31 White, H. J., "International Representation of the Surface Tension of Water Substance," Office of Std. Ref. Data, NBS, Washington, D. C., Dec. 1976.

32 Radovcich, N. A., and Moissis, R., "The Transition from Two-Phase Bubble Flow to Slug Flow," MIT Report 7-7673-22, 1962.

33 Henry, R. E., and Fauske, H. K., "The Two-Phase Critical Flow of One Component Mixtures in Nozzles, Orifices, and Short Tubes," ASME JOURNAL OF HEAT TRANSFER, Vol. 93, No. 2, May 1971, p. 179.

34 Grolmes, M. A., and Fauske, H. K., "An Evaluation of Incomplete Phase Separation in Freon Vented Depressurization Experiments," 3rd Multiphase Flow and Heat Transfer Symposium, Miami, Fla., Apr. 18-20, 1983.